SAE AERO DESIGN REPORT

FAMU-FSU College of Engineering
Team #37

Group Members:

Nestor Aguirre

Leah Evans

Martina Kvitkovicova

David Litter

Hebert Lopez

Zac Silver

STATEMENT OF COMPLIANCE

Certification of Qualification

Team Name	FAMU/FSU College of Engineering
Team Number	37
School	Famu-FSU College of Engineering
Faculty Advisor	CHIANG SHIH
Faculty Advisor's Email	Shih@eng.famu.fsu.edu

Statement of Compliance

As faculty Adviser:

CS (Initial) I certify that the registered team members are enrolled in collegiate courses.

CS (Initial) I certify that this team has designed and constructed the radio-controlled aircraft in the past nine (9) months with the intention to use this aircraft in the **2020** SAE Aero Design competition, without direct assistance from professional engineers, R/C model experts, and/or related professionals.

CS (Initial) I certify that this year's Design Report has original content written by members of this year's team.

CS (Initial) I certify that all reused content have been properly referenced and is in compliance with the University's plagiarism and reuse policies.

CS (Initial) I certify that the team has used the Aero Design inspection checklist to inspect their aircraft before arrival at Technical Inspection and that the team will present this completed checklist, signed by the Faculty Advisor or Team Captain, to the inspectors before Technical Inspection begins.

CS — Signature of Faculty Advisor — 1/22/2020. — Date

— Signature of Team Captain — 1/22/2020 — Date

Contents

List of Figures

List of Tables

Nomenclature

Table 1: List of Symbols and Acronyms

Symbol	**Description**
L	Lift & control surface length
T	Torque
F	Static thrust
C	Control surface
V	Velocity
α	Angle of attack
C_l, C_L	Coefficient of lift
C_d, C_D	Coefficient of drag
C_m , C_M	Coefficient of moment
C_{Lmax}	Maximum coefficient of moment
s_1	Maximum control surface deflection
s_2	Maximum servo deflection
Acronym	**Description**
SAE	Society of Automotive Engineers
FAMU	Florida Agricultural and Mechanical University
FSU	Florida State University
3D	Three-dimensional
RC	Radio controlled
PLA	Polylactic Acid
CAD	Computer Aided Drafting
FFF	Fused Filament Fabrication
CG	Center of Gravity
CL	Center Line
CD	Drag Coefficient
MAC	Mean Aerodynamic Chord
FBD	Free Body Diagram

1 Executive Summary

The following report outlines the processes the team used to design and manufacture a radio controlled (RC) airplane for the Society of Automotive Engineers (SAE) Aero Design East competition. The airplane is predicted to able to carry a size five soccer ball, one pound of cargo, and takeoff in under 60 ft. The short takeoff distance is achieved by using an Eppler 423, a high-lift airfoil, for the airplane's 6-foot wing. To be innovative, the 5.3-foot-long, 12.75 pound airplane is primarily constructed out of light weight polylactic acid (PLA) filament, a 3D printing material. This material is 50% less dense than regular PLA filaments, reducing the total weight of the airplane to increase its performance. 3D printing also allowed the team to create the airplane with a printed internal structure and external skin in modular parts. Modular parts make it easier to repair and assemble than a traditional RC airplane. The design also features a front loading cargo bay, accessible by a hinged nose cone. We used various programs to determine the data needed to create an airplane that is successful at competition and to also design the airplane itself: SOLIDWORKS, XFLR5, MATLAB, PropCalc 3.0, and Cura. The team's design focuses on using additive manufacturing to prove that the technologies are applicable to the RC airplane community. The team's primary focus for the competition was to showcase this innovative approach to design and manufacture an RC airplane with as much additive manufacturing as possible, realizing that this is not the conventional approach to the competition. The team's airplane design can be seen in Figure 1.

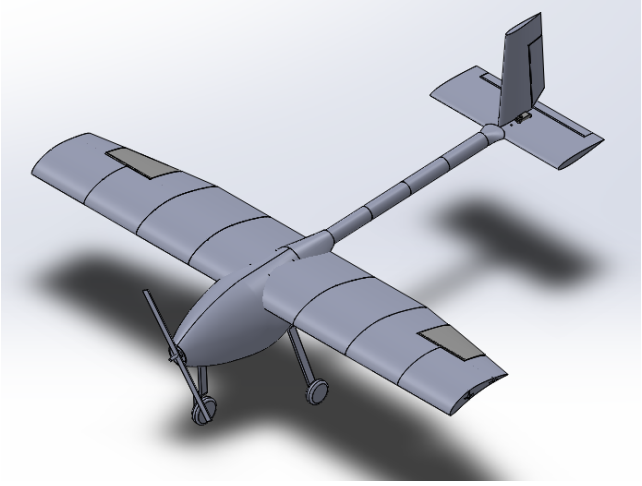

Figure 1: CAD model of airplane with modular pieces secured together

2 Schedule Summary

The team, composed of four mechanical engineering students and two electrical engineering students, was assigned to this project in September 2019. Roughly one third of the available time until competition was devoted to each stage of the design process: research, develop, and implement. The schedule was created after preliminary research and development was done based off of the major components of the airplane. Each team member was then assigned to research a specific component of the airplane such as: wings, fuselage, tail, thrust, landing gear, and electronics. Once research was underway, we adjusted the schedule to allow time to design, 3D print, assemble, and test the airplane before traveling to the competition in March 2020.

3 Table of Referenced Documents, References, and Specifications

Table 2: Table of References

Reference	Description
(n.d.). Servo Torque Calculator. Retrieved January 18, 2020, from http://www.mnbigbirds.com/Servo Torque Caculator.htm	Purpose: Formula for calculating servo torque Section(s): 6.2.2
Airfoiltools.com.(2020). Retrieved October 2019, from http://airfoiltools.com/airfoil	Purpose: Airfoil database for analysis Section(s): 4.2.2
Benson, T. (2014, June 12). Earth Atmosphere Model - English Units. Retrieved January 20, 2020, from https://www.grc.nasa.gov/WWW/K-12/rocket/atmos.html	Purpose: Density Altitude calculation for payload prediction Section(s): 6.2.5
Drive Calculator. (n.d.). Retrieved from http://www.drivecalc.de/	Purpose: Thrust calculations Section(s): 6.2
Lennon, A. (1999). Basics of RC model aircraft design: practical techniques for building better models. Ridgefiled, CT: Air Age Inc.	Purpose: Vehicle design configuration research, wing sizing calculations, and center of gravity calculations. Section(s): 4.2.2, 4.2.3, 4.2.4, 4.3.1, 4.3.2, 6.2.1, 6.2.3
Model Aircraft Power System Selection Using Your Computer. (n.d.). Retrieved from http://www.motocalc.com/tutorial/index.htmldifficult	Purpose: Thrust calculations Section(s): 6.2
Nicolai, L. M., and Carichner, G. (2010). Fundamentals of aircraft and airship design Volume 1, Aircraft design. Reston, VA: American Institute of Aeronautics and Astronautics.	Purpose: Lift, drag, and takeoff calculations. Section(s): 6.2.2, 6.2.3
Past Weather in Lakeland, Florida, USA - March 2019. (n.d.). Retrieved from https://www.timeanddate.com/weather/usa/lakeland/historic?month=3&year=2019	Purpose: Past weather averages for comparison of location Section(s): 5.2
Staples, G. (1970, January 1). Propeller Static & Dynamic Thrust Calculation - Part 2 of 2 - How Did I Come Up With This Equation? Retrieved from https://www.electricrcaircraftguy.com/2014/04/propeller-static-dynamic-thrust-equation-background.html	Purpose: Thrust calculations Section(s): 6.2

4 Design Layout & Trades

To gain a better understanding of the nuances of designing an RC airplane, the team completed a functional decomposition. We collaborated to create the functional decomposition utilizing our knowledge of physics and RC airplanes. This collaboration occurred as a team brainstorming session using a whiteboard to transcribe ideas. First, the major systems were identified by considering what the airplane must do fundamentally; that is to takeoff, land, and maintain flight all while carrying the designated payload. These fundamental tasks were identified as the major systems of the airplane. The minor systems were then identified based on the actions required to carry out the major functions. Highlights of the minor systems include the need to accelerate, generate lift, maneuver in flight, and carry a payload. Figure 2 displays the hierarchy chart created from the functional decomposition.

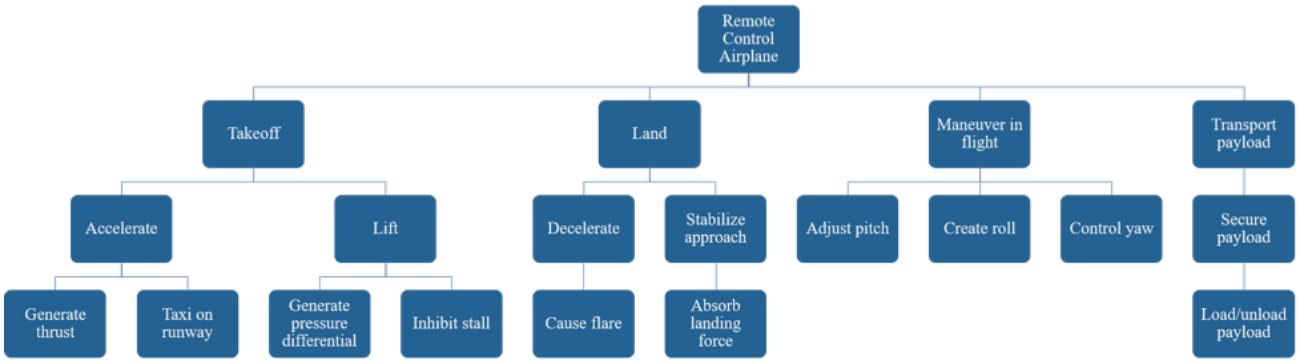

Figure 2: Functional decomposition hierarchy of airplane for competition

We deemed that the mission critical design metrics of the airplane are the wingspan, gross takeoff weight, coefficient of lift, and the thrust requirement. Each of these variables are dependent on each other and must balance as a system to achieve a successful takeoff, flight, and landing. Keeping the wing span of the airplane to less than 7 ft, the empty airplane weight to less than 20 lbs, and obtaining a lift coefficient greater than 1.0 are taken to be the mission critical targets. These targets, along with the thrust force, of the airplane are interdependent as the weight of the plane dictates the minimum values of the other targets. The necessary thrust force and the coefficient of lift targets were determined through external resources, such as textbooks about

aerodynamics and aircraft design (Lennon, 1999; see also Nicolai 2010). The aforementioned design requirements were translated to a mission profile for each major component of the aircraft. The process used to achieve these design requirements as well as the resulting airplane design is outlined in the following subsections.

4.1 Overall Design Layout and Size

The dimensions of the overall airplane can be seen in Table 3.

Table 3: Overall Airplane Design Specifications

Component:	**Dimension:**
Wingspan	72.0 inches
Wing Root Chord Length	14.0 inches
Wing Tip Chord Length	10.0 inches
Propeller to Tail Length	63.5 inches
Propeller Size	18x10E
Airfoil	Eppler 423
Wing Area	936 in^2
Landing Gear	Non-retractable Tricycle

4.2 Design Details and Features

The following section further describes our design process and selected features of the airplane.

4.2.1 Propulsion System

The process to design the propulsion system started with picking a motor. Per the rules of the competition, it was known that the airplane could only have a single electric motor. It was also known that the motor was limited to a maximum of 1000 W of power. With these specifications, the team did some research and narrowed down the possible electric motors to two options: The Power 60 Brushless Outrunner Motor 400 Kv and the Power 90 Brushless Outrunner Motor 325 Kv. The primary factor used to pick the motor was the Kv rating. Low Kv motors are good for slower flying airplanes because a lower kV rating corresponds to a higher output torque. A higher output torque allows the team to use a larger propeller with a relatively small pitch; this is typical in short take off and landing airplanes. It was determined that the Power 90 Brushless

Outrunner Motor 325 Kv is the best option due to its lower Kv rating which is appropriate for for our application.

With the motor known, a suitable battery was researched. Per the rules of the competition, it was known that the battery had to be a commercially available 6S Lithium-Polymer battery and have a current carrying capacity of at least 3,300 mAh. With the power known (power limited to 1000 W by the power limiter) and knowing that the battery must be 6S (22.2 V), it was determined that the maximum required current is 45.05 A. The battery must be able to deliver this much current to the airplane. With these constraints, the team came up with two options for batteries: (1) Onyx 22.2 V, 4000 mAh, 6S 30 C, LiPo Battery, and (2) an Admiral 4500 mAh, 6S, 22.2 V, 40C LiPo Battery. Generally, a higher discharge rate is good because it gives a higher maximum discharge current, however, it is not necessary since the power is limited to 1000 W. Therefore, a lower discharge rate is preferred since it will deliver the amount of power needed. Additionally, to keep the weight down, only the essential amperage of the battery is desired since a higher mAh causes the battery to be heavier; sometimes up to a half pound heavier. Based on this, the team decided to use the Onyx 22.2 V, 4000 mAh, 6S, 30 C LiPo Battery. By multiplying the C rating with the 4 A it was calculated that this battery can deliver a maximum of 120 A. It is predicted that this battery will allow for 5.33 minutes of flight time. If 20% of the charge is left within the battery, as recommended, the airplane will have a flight time of 4.26 minutes.

4.2.2 Airfoil

The team researched the airfoil tools database for airfoils that would satisfy the mission profile of preforming well in low Reynolds numbers and having a gentle stall, high lift, and a moderate pitching moment. Two under-cambered airfoils, the Selig 1223 and Eppler E423, and two modified flat bottom airfoils, the Clark-Y and NACA 4412, were analyzed at a Reynolds number of 200,000. Figure (3) below compares the behavior of the selected airfoils for C_l/C_d, and C_m versus α. Symmetric airfoils were not considered because aerobatic maneuvers will not be performed.

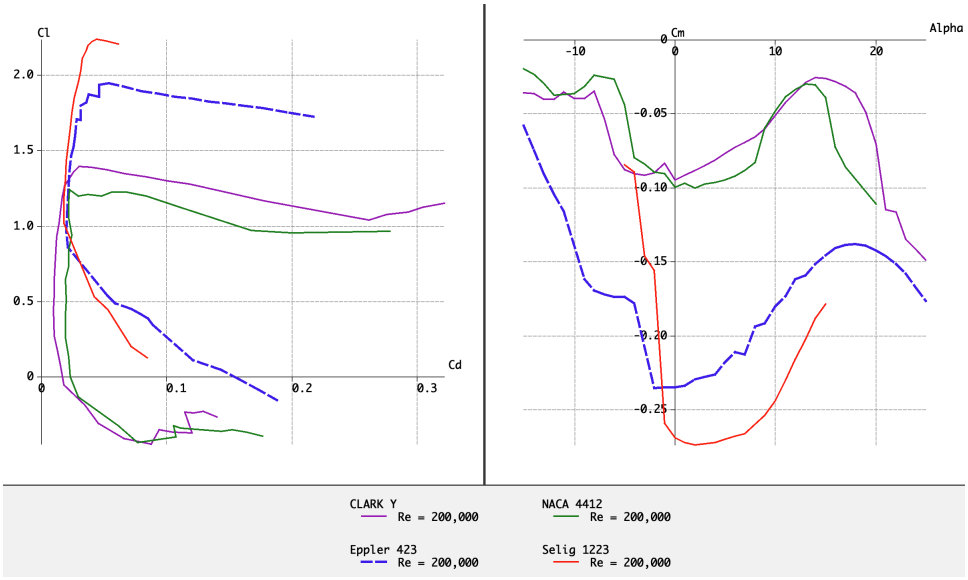

Figure 3: Airfoil data at a Re of 200,000 over a range of angles of attack that were analyzed to select the best airfoil for competition

From Figure 3, it can be seen that the under-cambered airfoils' maximum lift coefficient is nearly double the modified flat bottom when the airfoils are plotted against their C_d values. Despite displaying the desired quality of a moderate pitching moment and gentle stall, the Clark-Y and NACA 4412 airfoils were eliminated because of their low lift coefficient. When the C_l/C_d versus α data of the airfoils were compared, the Eppler E423 and Selig 1123 had a comparable maximum C_l/C_d. When the moment coefficient versus alpha of the airfoils is compared in Figure 3, the Eppler E423 is found to have a more positive and favorable C_m by approximately 0.05. Although a small difference, this behavior affects the sizing of the horizontal stabilizer to balance the moment of the airplane; the more negative C_m is, the larger the horizontal stabilizer must be, thus increasing the weight of the airplane. Considering manufacturing needs, the Eppler E423 is also favorable because it has thicker trailing edge which increases the success of a strong 3D printed cross section. Ultimately, the Eppler E423 airfoil was chosen because it fit the teams competitive needs the best.

4.2.3 Wing Planform

Research through Andy Lennon's "Basics of RC Aircraft Design" provided insight on performance differences between various wing planform styles. The wing planform has a mission

profile of uniform lift, stable flight, and low drag. Five wing planforms were researched: (1) rectangular, (2) leading edge taper, (3) trailing edge taper, (4) leading and trailing edge taper, and (5) elliptical. For the benefit of increased stability and maneuverability a high wing was selected.

From research and analysis, it was found that the elliptical wing met the mission profile with the highest C_L/C_D value of 27 at 0 degrees alpha; however, it was eliminated as a choice due to the variable chord length that increases the design and manufacturing complexity. A rectangular wing yields the opposite result with the lowest C_L/C_D value of 21 at 0 degrees alpha, but the constant chord length simplifies design and manufacturing complexity. The tapered wings are considered to be a mix of the extremes of a rectangular and an elliptical wing. Furthermore, we found that the rectangular and tapered wings produced smaller C_M values. This lead the team to research and select a sixth wing planform for our design: a combination of a rectangular and tapered wing. Discussion of the optimization of wing planform is further detailed in Section 4.3.1.

4.2.4 Landing Gear

The type of landing gear an airplane utilizes effects its performance and controllability during takeoff and landing. Therefore, it was critical to gain an understanding of these effects through research using Andy Lennon's "Basics of RC Aircraft Design". The team considered two styles of landing gear: (1) tricycle and (2) tail-dragger landing gear. We then analyzed which would yield better performance and controllability during takeoff and landing. A summary of our research is shown below in Table 4.

Table 4: Comparison of Landing Gear Style

	Advantages	**Disadvantages**
Tricycle Landing Gear	• CG behind main wheels • Steerable nose wheel • Increased stability during takeoff	• Increase weight from three large wheels • Requires increased skill level for landing
Tail-dragger Landing Gear	• Aesthetics • Decreased weight from two large and one small wheel • Requires moderate skill level for landing	• CG behind main wheels • Increased instability after tail wheel lifts off ground • Relies on rudder control • Prone to nose tip over

A tricycle landing gear configuration was selected for the advantages of increased stability during takeoff due to the position of the wheels in relation to the CG. This in combination with having the ability to steer without using the control surfaces was deemed as an advantage over the tail-dragger configuration.

4.3 Optimization

4.3.1 Optimization and Sensitively Analysis

After selecting the wing planform design, further optimization was required to meet the mission profile and manufacturing requirements. A wing with 50% rectangular and 50% trailing taper wing results in a straight leading edge which allows the usage of a support spar at the mean aerodynamic center for the span of the wing. Furthermore, it optimizes the 3D printing process by reducing the number of unique wing sections that need to be created. Using the program XFLR5, we performed an analysis on several taper ratios for a 50% rectangular and 50% trailing edge taper wing planform. Figures 4 and 5 below display these results.

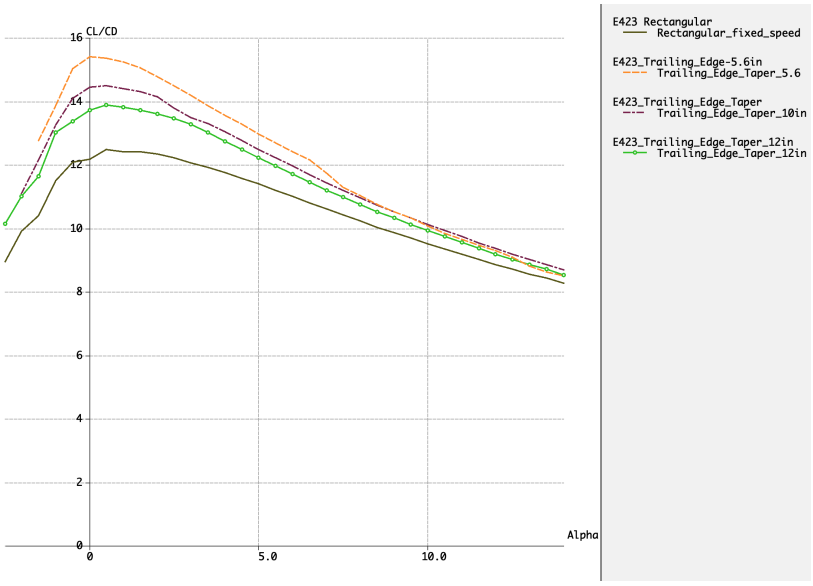

Figure 4: The C_L/C_D as a function of the angle of attack for different leading edge taper ratios

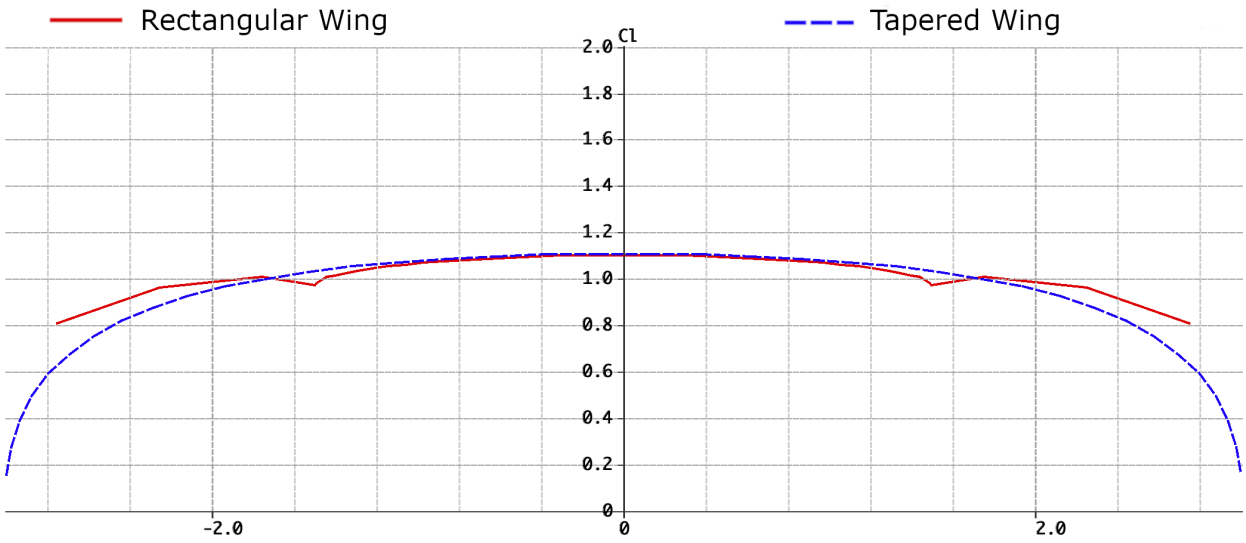

Figure 5: Spanwise distribution of lift on a rectangular and tapered wing

Figure 4 shows how a more significant taper increases C_L/C_D from a value of 12 to 15 across lower angles of attack; however, this increase in C_L/C_D results in an increase in the speed that is needed to take-off and cruise because the overall lift that is generated by the wing is decreased. . Research by Lennon also suggests this more gradual taper will yield better performance by means of more stable flight. Sharp taper ratios typically result in aerobatic airplanes, which is not our mission profile. Because of this, the 14 in to 10 in taper that begins at half of the wing was found to be an ideal balance between lift and efficiency. Figure 5 shows how the lift value at the wing tip increases from 0.2 to 0.8, displaying the spanwise distribution of lift as more uniform on a tapered wing compared to a rectangular wing.

With the wing planform selected, a MatLab script was created for optimizing the wingspan for a competitive takeoff performance. An iterative process was used to solve for the chord length, wingspan, and wing planform required to achieve the target gross takeoff weight of 15 lbs and under 100 ft takeoff distance. Wing planform area, which is a product of wingspan and chord length, was found to be the most sensitive variable for satisfying takeoff requirements because it is included in the equation for lift and takeoff velocity. Our team is constrained in chord length by the 3D printing manufacturing process because of the size of the 3D printing bed; therefore, we were restricted to a maximum chord length of 14 inches to avoid printing a separate leading and trailing edge airfoil rib. Desiring to design an airplane fitting the mission profile of a stable

slow flying airplane resulted in a target of wing loading of 20 oz/ft^2. Due to the the constraints of 3D printing, our design has a wing loading of 36 oz/ft^2. However, with a wingspan of 72 inches we predict our airplane will still perform to a satisfactory standard of maneuverability.

4.4 Interfaces and Attachments

To create the larger components of the airplane, the 3D modular pieces are secured together using several different methods. The modular pieces of the airplane vary in both size and shape and use different connections throughout the plane to construct different components of the airplane. The wings, as mentioned before, use two aluminum spars to secure the 9 in sections of the wing together under compression with the use of fasteners at each wing tip. The wing as a whole is secured to the fuselage through a form fit on top of the fuselage along with fasteners. The servos within the wings are secured within their housings using screws that are tightened directly in 3D printed holes within the servo housing. Other smaller modular pieces are also secured with small screws that are screwed into 3D printed material. Glue is used sparingly around the airplane; this was done in an effort to make it easy to replace components if components are damaged.

5 Loads and Environments Assumptions

The following subsections explain the various design loads that the airplane will be subjected to in flight. Detailing the loads that will have the greatest impact on the airplane. Moreover, there is another section of the report that considers the weather conditions to provide the team with a general idea of the weather.

5.1 Design Loads Derivations

There are multiple loads acting on an aircraft such as lift, weight, drag, and thrust. The thrust performance was analyzed to confirm that the airplane will have enough force to move the airplane in air and produce lift. Thrust must overcome the drag and weight of an airplane. The

lift characteristics was obtained using thrust calculations to find the velocity needed for takeoff. The strongest impact that will be done to the airplane while in flight will be due to the landing as the force will have to be absorbed by the landing gear. This can cause a failure and potential risk to the plane. Due to this, students have chosen a durable material to represent the landing gear that will be able to withstand a hard landing. During takeoff, the wings will have to absorb a lot of force while producing lift, therefore, as mentioned previously, the team decided for a structural addition in the form of an aluminum spar running along both wings and through the fuselage.

5.2 Environmental Considerations

The competition is being held in the same state as where the team is from, therefore similar weather conditions are anticipated. The past weather conditions between Tallahassee and Lakeland were looked at for the month of March. In March, the weather averages show only a few degrees difference with one less rainy day recorded (TimeandDate.com, 2019). The students assume the conditions for the competition will not have any crosswind, headwind, tailwind, or downdraft. Due to the aircraft being roughly 15 lbs, it is suitable for outdoor flight under normal wind conditions. The aircraft will undergo a series of tests for correct working condition after construction, therefore it will be able to perform to the highest standard while at the competition.

6 Analysis

The analysis of the airplane structure and its performance were analyzed using computer software, hand calculations, and physical testing. Different analyses were used to verify the theoretical performance of the airplane. Throughout the analysis, factors of safety were used to ensure that the airplane would satisfy the competition requirements, even in adverse conditions. The various analysis tools and methods allowed for us to iterate the size, shape of different components of the airplane.

6.0.1 Analytical Tools

Various programs such as SOLIDWORKS, XFLR5, MATLAB, PropCalc 3.0, and Cura were used when needed. XFLR5 was used to compare various airfoils and generate graphs regarding coefficients of lift, drag, and moment. PropCalc 3.0 was used to determine the thrust provided based on motor values and various propellers. MATLAB was used to calculate the expected take off distance, drag, lift produced, the weight of the airplane, for stability and controls. SOLIDWORKS was used as the CAD program to design the entire airplane; the center of gravity was calculated using SOLIDWORKS. Cura was used to slice the segments of the airplane to be 3D printed on the team's Lulzbot printer.

6.1 Performance Analysis

In order to get a more accurate idea of the propulsion system of the airplane, we built a thrust stand to test the entire system functionality and to identify which propeller generates the most static thrust given our electrical setup. Prior to testing all propellers were balanced. Figure 6 shows the thrust stand that was used to test different propeller pitches and sizes. Three propellers manufactured by APC were tested using this setup: (1) 16x8E, (2) 18x8E, and (3) 18x10E.

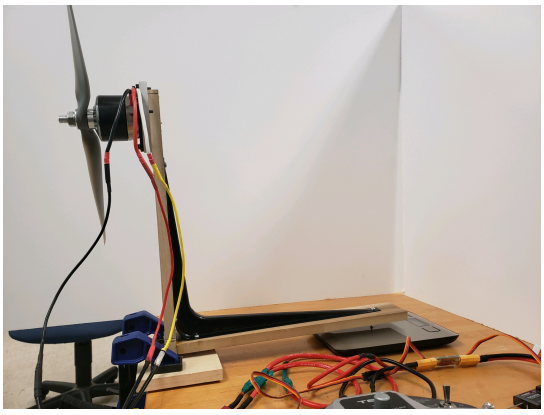

Figure 6: Thrust stand

The thrust stand consists of two arms with a common pivot. The motor is located on the vertical arm and a scale is located below the horizontal arm. The distance of where the scale and thrust stand meet is the same distance from the pivot point as the center of thrust. This simplified the

analysis as the thrust generated by the motor can be assumed to be the reading on the scale. The static thrust test was performed with all the electronic components that will be used in the airplane, including the power limiter. From the test it was found that the maximum static thrust at full throttle for the 16x8E, 18x8E, and 18x10E was 7.694 lbs, 9.331 lbs, and 10.011 lbs, respectively. Once the static thrust was determined, equation 1 was used to determine how thrust varies with increasing velocity (Gabriel Staples – Propeller Static Dynamic Thrust Calculation). The results of this analysis is discussed in the next section.

$$F = \frac{1.225(0.0225d)^2}{4}\left((RPM)(0.0225)(pitch)(\frac{1min}{60sec}\right)^2 \tag{1}$$

6.1.1 Runway/Launch/Landing Performance

With the output of the propulsion system known, an estimation of takeoff performance can be found. The net thrust of our airplane was found by subtracting drag force from the dynamic thrust. Figure 7 shows our airplane theoretical performance, it assumed to be a close approximation of the flight performance of our selected 18x10E propeller.

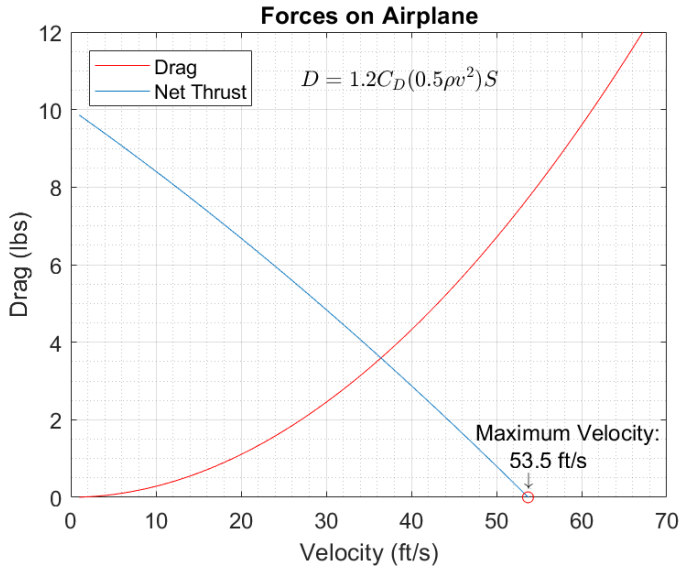

Figure 7: Performance Prediction: Drag and Thrust versus Velocity

Finding the equilibrium point of the forces of thrust and drag results in the maximum obtainable velocity of our airplane in flight: 53.5 ft/s or 36.5 mph. This value is important because it

showcases the maximum capability of our design.

Referencing Lee Nicolai's White paper and the thrust calculations from the previous section, the lift and velocity required for takeoff was determined. The required equation and result of these calculations is shown in Figure 8 below (Lennon, 1999; see also Nicolai 2010).

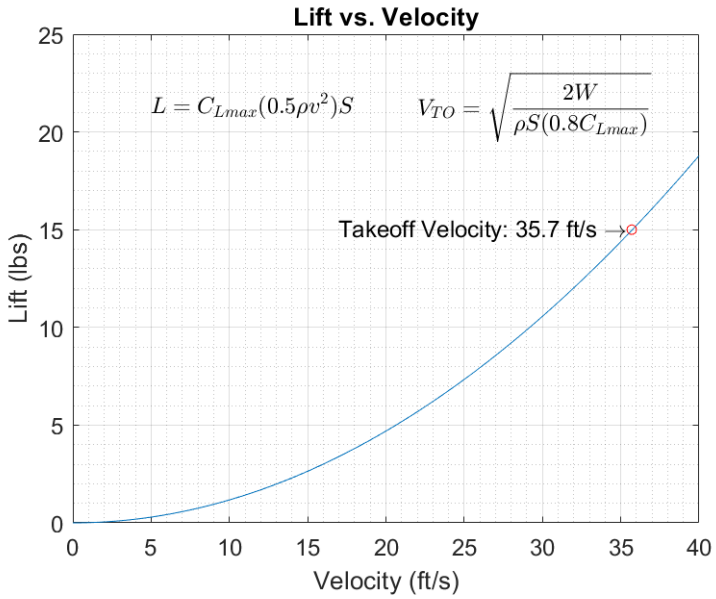

Figure 8: Performance Prediction: Generated Lift versus Velocity

When the generated lift force equals the weight of the airplane, takeoff will occur. Our airplane is designed to have a total loaded weight of nearly 15 lbs and takeoff at a velocity of 35.7 ft/s or 24.3 mph after traveling 53.4 ft. The required takeoff distance includes almost a 50% safety margin to account for added weight as a result of manufacturing while providing the option of carrying more steel plates, if feasible.

6.1.2 Flight and Maneuver Performance (Incl. Surface Sizing)

To be able to control the aircraft to the highest precision during flight, a performance analysis was made to ensure the 3D printed airplane will be able to maneuver correctly while both in air and on the ground. For optimum performance of an airplane, the servos must be sized correctly. The team obtained the servo's torque from the given technical data table that came with the servo motors. The torques on the data sheet were confirmed through calculations. The torque

values needed to move the control surfaces were calculated using the equation 2.

$$T = 8.5 * 10^{-6} \left(\frac{C^2 V^2 L sin(s1) tan(s1)}{tan(s2)} \right) \tag{2}$$

The equation represents C for control surface chord in cm, V for speed in mph, L for control surface length in cm, s_1 for maximum control surface deflection in degrees, and s_2 for maximum servo deflection in degrees. The equation produces a numerical answer in oz-in. and automatically converts centimeters to inches. The maximum control surface deflection is 35 degrees and maximum servo deflection is 40 degrees.

Figure 9: Servo torque that is necessary for different control surfaces on the airplane

The following results for aileron, elevator, and rudder are 20.2, 21.6, and 9.19 oz-in, respectively under normal conditions. During flight, the expected speed is roughly 30 mph, however, during a windy day, the speed could increase up to 45 mph. The torque values necessary to move the control surfaces would change to 45.4, 48.5, and 20.0 oz-in for aileron, elevator, and rudder, respectively. The calculated torques ensure that the servos were sized correctly and should handle any situation they face during flight. In the graph above (Figure 9), the team shows a comparison of servo torque needed during various speed conditions including wind and free-fall which would occur at 55 mph. The servos used are rated to 83.3 oz-in and are powered by a separate 6 V battery. While the airplane is in air flying, all four forces are acting on it, meaning that the

lift needs to balance its weight and the thrust produced balances the drag. At this condition, the airplane is flying at a non-variable speed in a straight pattern. During flight, the forces change as the plane changes direction. The plane must fly at a minimum speed of 25 mph for the velocity to maintain the current flight altitude while the maximum velocity in flight is 36.5 mph. Verification of these values is shown in the plots from Section 6.1.1

6.1.3 Dynamic & Static Stability

Figure 10 shows how the airplane's stability changes with varying the location of the center of gravity (CG); this plot was made using XFLR5. From Figure 4, we explored moving the location around 30% of the mean aerodynamic chord (MAC). From the Figure 10, we see that all three locations of the CG are stable to some degree as the slope of the lines are negative. We found that locating the CG at 35% would yield a positive moment coefficient at zero angle of attack. This is not ideal as this would cause the nose of the airplane to pull upwards while the airplane is level at cruising speed which could result in the airplane going into a stall. When the CG is 25% of MAC (red dashed line), we saw that the airplane has a negative moment coefficient. A negative moment coefficient is considered stable to a certain degree as the nose of the airplane naturally wants to tilt downwards. This is stable as when their is no input from the user, the nose of airplane will slightly tilt downwards and gain speed rather than going into a stall. However, a moment coefficient that is too negative will result in an airplane that is difficult to fly. A certain balance is needed to be achieved so that a great degree of user input is not needed to fly the airplane level. We decided to place our CG at 30% of the MAC because of this. We believe this will result in an airplane that is stable and easy to fly as the moment coefficient is slightly negative at zero angle of attack. The location of the CG will allow us to make slight trim adjustments to get the ideal stability of the airplane.

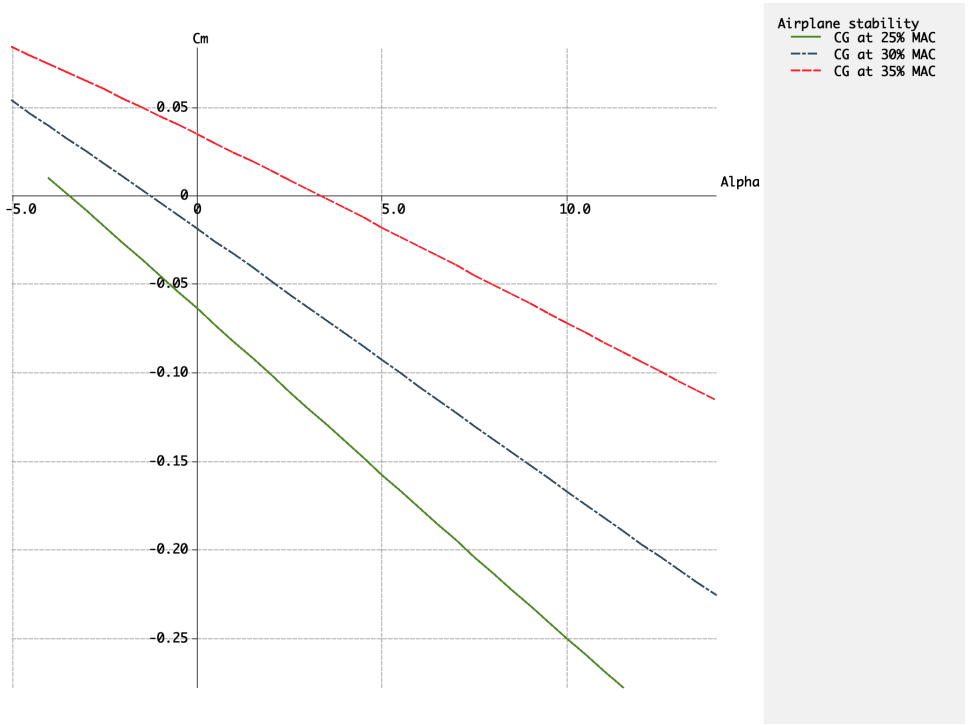

Figure 10: Moment coefficient vs. alpha that shows airplanes dynamic stability with changing the center of gravity position on the airplane

6.1.4 Aeroelasticity

An aeroelasticity study was carried out to ensure that the airplane would be able to withstand the fluid flow when in a static and dynamic environment. This is important because lightweight airplanes are exposed to larger aerodynamic forces. When designing our airplane we had to take into account divergence, control reversal, and flutter. Divergence occurs when the aerodynamic forces causes the wings angle of attack to change resulting in increased forces. Control reversal occurs when the activation of the control surfaces causes the inverse aerodynamic moment to occur. If this occurs, the control surfaces can reduce the effectiveness of the control. Finally, flutter is excessive vibrations that the airplane cannot handle resulting in the failure of the airplane. To test for fluttering of the wing design; the team plans to use one of the wind tunnels available to them on campus. We can use this test to determine the speed at which fluttering will begin to occur. Knowing the speed at which fluttering occurs helps us learn the limitations of our airplane.

6.1.5 Lifting Performance, Payload Prediction, and Margin

As previously mentioned in Section 5.2, the team has the advantage of similar environmental conditions between our university and location of the competition. This translates to roughly the same elevation between our location than the location of competition. However, if our airplane is required to fly at another elevation it is desirable to predict the expected performance by means of how much payload it can carry. To do this, the team found the linear relationship between payload weight and density altitude. The resulting plot does not account for local weather conditions or factors that may affect takeoff performance and is shown in Appendix A.

6.1.6 Applied Loads and Critical Margins Discussion

To simplify our analysis, the wing was simulated as a beam. The wing could generate a maximum of 22.5 lbs of lift traveling at maximum velocity. With a factor of safety of 1.2; the wing can generate up to 27 lbs of lift. The lift generated is distributed in two sections of the wing and the fuselage. The section of the fuselage that is connected to the wing varies in thickness, so we approximated an average thickness of 4 inches in between this two supports. Figure 11 shows the free body diagram of the wing. The weight of the fuselage which is around 15 lb acts on the two supports located at x = 34 in and x = 38 in

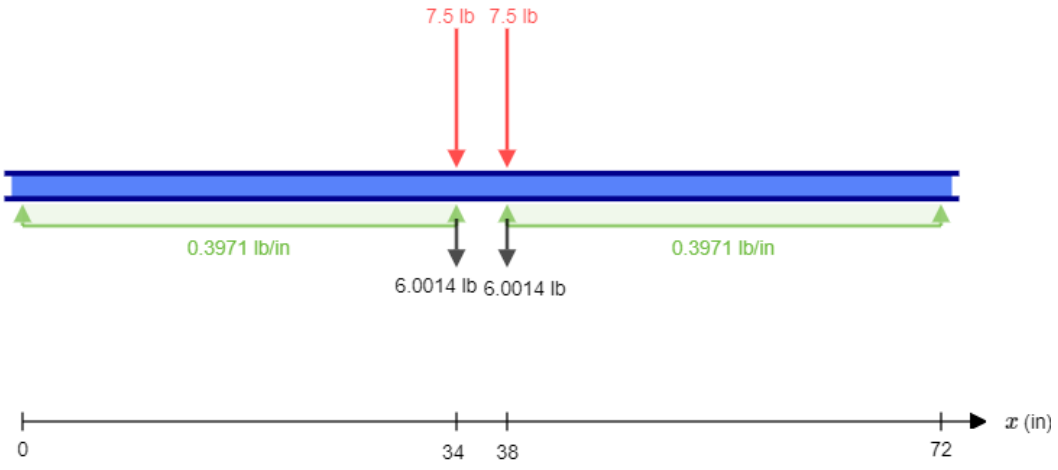

Figure 11: Free Body Diagram (FBD) wing

With the free body diagram we generated a shear force diagram that shows that the maximum shear force is 13.501 lb and a bending diagram with maximum bending of 229.524 lb-in

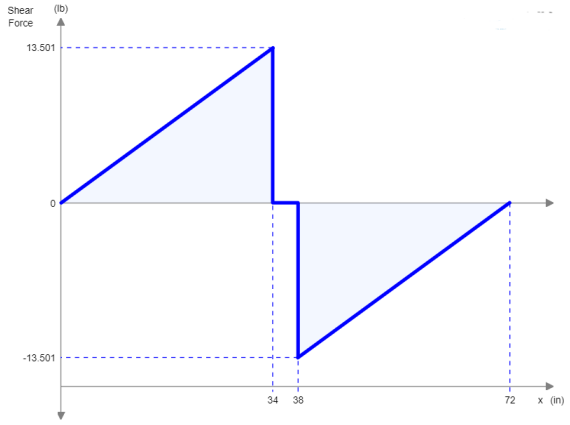

Figure 12: Shear Force Diagram

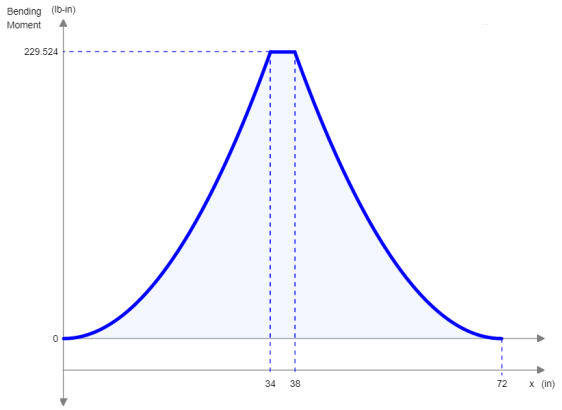

Figure 13: Bending Body Diagram

$$Margin\ of\ Safety = \frac{Allowable}{(Safety\ Factor * Actual) - 1} \tag{3}$$

7 Assembly, Test and Integration

7.1 Assembly

The airplane consists of modular pieces that need to be assembled together. Beginning with the wing; each piece is slid onto two aluminum spars that area used as supports. Half of the entire wing can be seen in Figure 14 below. The wings are put into compression by bolting end caps

Figure 14: 3D printed modular Wing

on each end of the wing. The bolts will go into the two aluminum spars. Next, the fuselage consists of three pieces. Each piece of the fuselage will have a lip that goes over the piece it

connects to. Glue will be placed under the lip which will ensure a good connection from piece to piece. Once the fuselage has been glued and is secured together. The wings will be slid through these cut out sections on the fuselage. The wings will then be bolted down to the fuselage to ensure that they are safely secured. The boom will be constructed by screwing the 3D printed modular cylinders together. The boom will be connected to the fuselage and tail by screwing it in with the spar running slightly into both parts. The tail will be printed in seven pieces. The horizontal tail will consists of three pieces with the elevator being the fourth. The three pieces will be screwed together and the elevator will be held in place by a 3D printed male and female hinge. The vertical tail will be three pieces. Two of the pieces will be the vertical tail that is split horizontally in half. The rudder will be attached to the vertical tail. The vertical tail and horizontal tail will be bolted together.

7.2 Test and Integration

The test and integration of the RC airplane involves a materials test, circuit test, and flight test. The materials test involves printing tensile specimens at variable infill to determine mechanical properties such as yield strength, ultimate tensile strength, and failure point. This will help us gain an understanding of the limitation of the material for RC airplane manufacturing. A circuit test has been conducted to ensure that all electrical components are fully operational and up to safety standards as stated by SAE. The test was done using a multi-meter to ensure that the correct currents and voltages are being measured all throughout the circuit. We also made sure the red arming plug is fully functional within our circuit. A flight test will be conducted once the airplane has been fully printed and completely assembled. The flight test will show us that the airplane was accurately designed and manufactured. We will check the manoeuvrability of the airplane. We will ensure the control surfaces are fully functional.

8 Manufacturing

Manufacturing the airplane out of 3D filament was found to have as many advantages as it did disadvantages over typical RC construction techniques. The filament that is used to make the airplane was found to be more difficult than expected to dial in the settings for the 3D printers that we were provided (Lulzbot Taz 6). The lightweight PLA filament that we used to construct our airplane foams to different degrees as it printed at different nozzle temperatures. To decrease the density of the 3D printed parts we wanted to maximize the degree to which the material foamed while it was printed. We found that at 230^{o}C the lightweight PLA increased its volume by 110% (temperature will vary based on the 3D printer that is used). Since the volume of filament extruded from the nozzle was increased, the flow rate of the filament fed through the nozzle needed to be decreased to ensure that our 3D printed parts would be dimensionally accurate. We found that by decreasing the flow rate of the filament through the nozzle by 50% resulted in parts that were dimensionally accurate. By reducing the flow rate of filament, a weight reduction of 50% is seen in all of the parts printed using the lightweight PLA filament over normal PLA.

Designing is a major challenge of using additive manufacturing techniques for production of the airplane. Designing parts that can be 3D printed is difficult because you must take into consideration how it will be printed, how the walls will print, how steep the angles are, and how the parts can be placed on the print bed to be printed. To design these parts requires thinking in negative space, which is not conventional.

9 Innovation

We approached this competition with the mindset of innovation. The decision of using the additive manufacturing technique — fused filament fabrication — created a new challenge when it came to designing. The material used to create the airplane is lightweight PLA. A major challenge of going with this method is that our airplane has to be constructed in modular pieces. Each modular piece needs to be able to be 3D printed and assembled. Therefore, when design-

ing it is necessary to account for the print-ability. Moreover, the cargo bay features a guppy design. A guppy design involves a split of the fuselage from the nose to wing that swings open parallel to the ground once unconstrained. This is not a common method for accessing cargo when it comes to RC airplanes. We used this access method to be as innovative as possible and push the boundaries of RC airplane design.

10 Conclusion

This RC airplane has gone through multiple iterations of design, analysis, and soon testing. The airplane features a unique swinging hatch for front loading the cargo bay, a wing that slides through the fuselage, and a 3D printed internal structure and external skin. We believe that our airplane represents the culmination of our learning here at the FAMU-FSU College of Engineering. The design of this RC airplane is meant to highlight the techniques of additive manufacturing for airplane manufacturing. We hope to show that 3D printing is a valid technique and aim to inspire others to take on the challenge.

SUMMARY DATA	
WINGSPAN	72IN.
EMPTY WEIGHT	12.75LB
BATTERY CAPACY	6s LIPO 4000MAH
MOTOR MAKE/MODEL	E-FLIGHT Power 90 BRUSHLESS
MOTOR KV	325
PROPELLER	APC 18X10E
SERVO	HI-TEC HS-485HB 83.3 OZ-IN

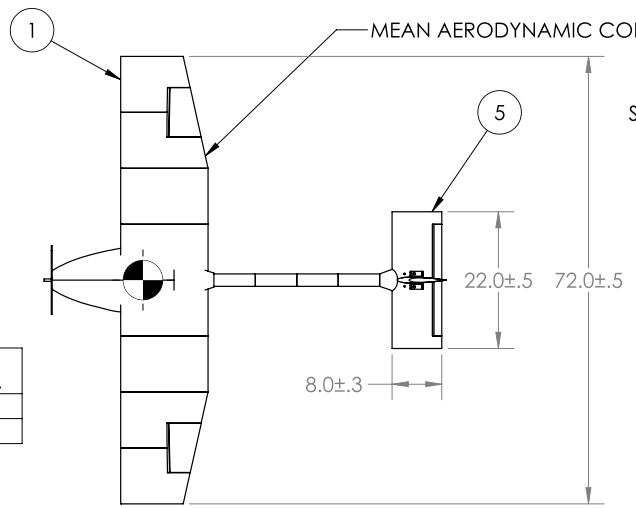

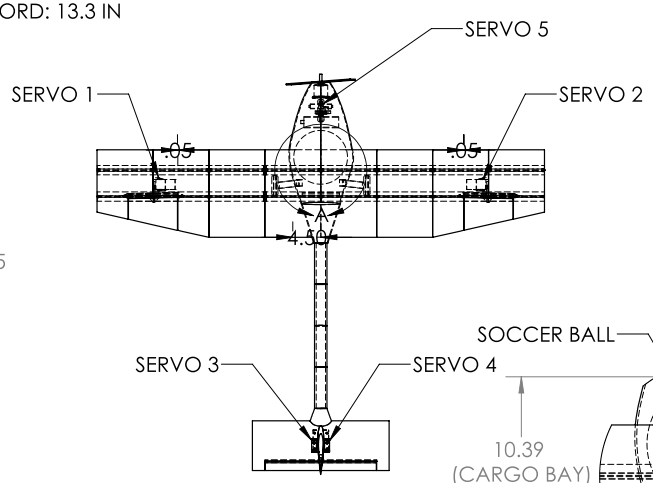

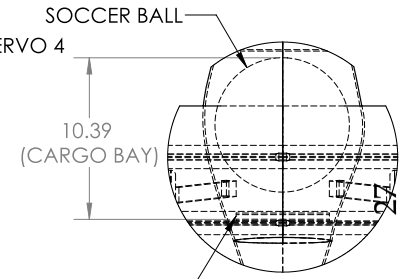

DETAIL A
SCALE 1 : 8

	STATIC MARGIN	CG LOCATION FROM DATUM A
UNLOADED	0.12	14.73
LOADED	0.12	14.73

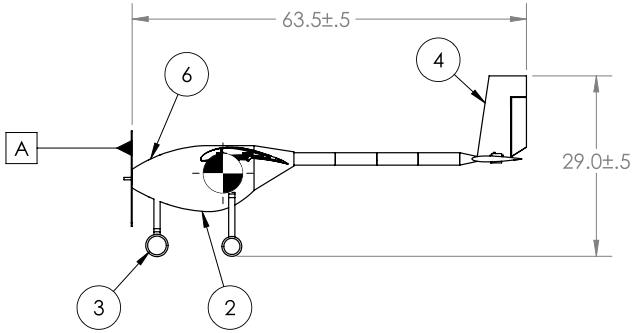

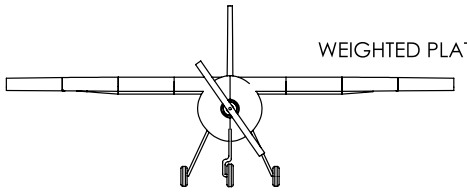

WEIGHT AND BALANCE			
ITEM	X DISTANCE FROM DATUM A (IN.)	WEIGHT (LB)	MOMENT FROM DATUM (IN-LB.)
SERVO 1	16.83	0.0993	1.67
SERVO 2	16.83	0.0993	1.67
SERVO 3	58.12	0.0993	5.77
SERVO 4	58.12	0.0993	5.77
SERVO 5	4.68	0.0993	0.46
ESC	3.98	0.1656	0.66
RECIEVER	5.13	0.0175	0.09
MOTOR	1.58	0.9880	1.56
BATTERY	6.49	1.2750	8.27
PAYLOAD (SOCCER BALL)	12.20	1.0000	12.20
PAYLOAD (WEIGHTED PLATE)	17.90	1.0000	12.20

SUBASSEMBLIES	
BALLOON #:	ITEM
1	WING
2	FUSELAGE
3	LANDING GEAR
4	VERTICAL STABILIZER
5	HORIZONTAL STABILIZER
6	NOSE CONE

DRAWN BY: ZAC SILVER	TEAM #: 37
MATERIAL: LIGHTWEIGHT PLA ALUMINUM	TEAM NAME: FAMU-FSU College of Engineering
NOTES: NOT TO SCALE	SCHOOL NAME: FAMU-FSU College of Engineering

Appendix A - Technical Data Sheet

Team Name: FAMU/FSU College of Engineering

School Name: FAMU-FSU College of Engineering

Team Number: 37

Shown below is the plot of density altitude versus weight of the airplane, depicting the predicted payload capacity of the airplane. The steps taken to create this plot are discussed in Section 6.1.5.

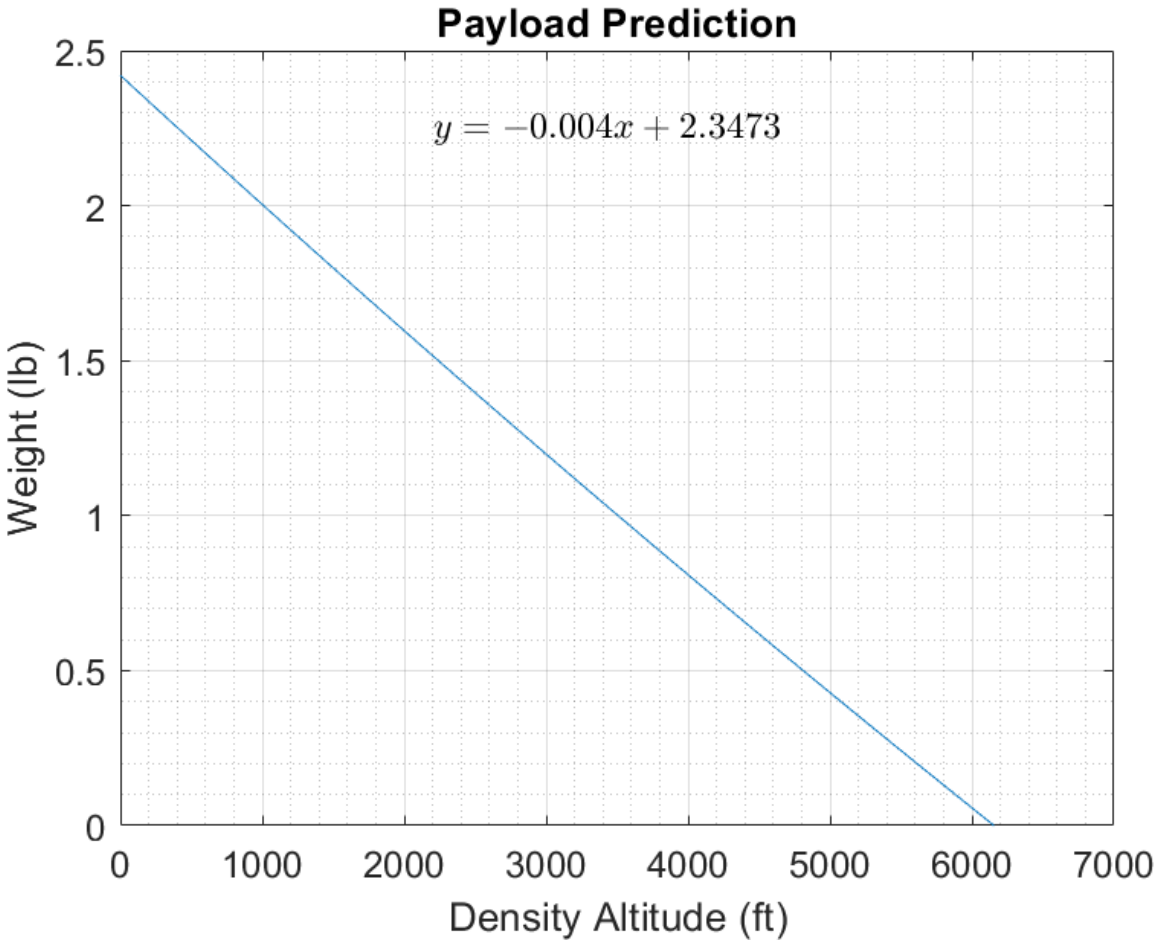

Payload Prediction: Cargo Capacity as a Function of Altitude